

# Serpentine motion control of snake robots for curvature and heading based trajectory – parameterization

Eleni Kelasidi and Anthony Tzes

**Abstract**—The control problem for the serpentine motion of a planar snake under the assumption of a trajectory characterized by its curvature and heading is examined in this article. The time varying curvature and heading attributes of the trajectory result in a sinusoidal reference signal for the joint angles. An inner loop PD-controller is used for trajectory tracking by compensating the effects of the snake’s dynamics, while an outer loop first-order controller is used for the formation of the reference joint angles by tracking the desired heading and velocity. Simulation studies on spiral curves are included to investigate the efficiency of the controller.

## I. INTRODUCTION

Snake-like robots have been studied due to their ability to move in difficult environments, where other types of robots, usually, fail. Empirical and analytical studies of snake locomotion were reported by Gray [1]. Among the first attempts to develop a snake prototype, the work of Hirose [2] is essential. Snake robots have a high number of Degree of Freedom (DOF), and are capable of moving without the use of legs or wheels. The multitude of DOF of snake robots makes it difficult to be controlled, but provides the ability of traversing in irregular environments, something that surpasses the mobility of the conventional wheeled, tracked and legged types of robots [3].

Mathematical descriptions of the forces acting on a snake are proposed in [1] and used to re-enact the attributes of snake locomotion. It is shown that the forward motion of a planar snake, requires the existence of external forces that act in the normal direction to the snake’s body. Hirose [2] studied biological snakes and modeled the snake’s body as a continuous curve that could move sideways (sideslip constrains); the serpenoid curve was then formulated, which is a mathematical description of lateral undulation (the most common form of snake locomotion). Hirose found out that a close approximation to the shape of a biological snake, during lateral undulation, is given by a planar curve with its curvature varying sinusoidally.

The dynamics of the snake robots are derived by utilizing various modeling techniques [3]. For the case of wheel-less snake robots, the friction between the snake robot and the ground, affects significantly its motion. In addition to many models of snake robots that consider sideslip constraints,

there have been reported cases with anisotropic ground friction properties similar to biological snakes, providing the opportunity to model lateral undulation locomotion patterns. The modeling and control issues including in ground friction the viscous and Coulomb friction terms, were presented in [4]. In most of the simulated gaits, with the inclusion of a viscous snake-to-ground friction model, the condition that the tangential friction is less than the normal-friction was necessary, for the case of a lateral undulation relying on the anisotropic friction properties. Many types of controllers are proposed in the literature focusing on the path tracking control issue. Directional control during lateral undulation is considered in [5, 6]. The works [7, 8] propose path following controllers for three-linked and four-linked wheeled snake robots based on Lie bracket theory, while the more recent ones examine the controllability of these robots. A straight-line path following controller for planar snake robots is considered by the authors in [9, 10], while in [11], a genetic-tuned path-planning controller is proposed for a serpenoid-motion. A tracking control method, relying on sensor information, is presented in [6], while [12] proposes a path planning motion, based on the artificial potential method. Moreover, [13] gives a computational model for amplitude modulation of the control effort for the case of a path with turns. Assuming a serpenoid curve, the authors in work [14] propose a method to control the snake robot motion in a prescribed path. The authors utilize the curvature path of a snake-like robot and in the presence of Coulomb friction, the robot travels on prescribed curvilinear and linear paths. In [15], the control architecture is based on a central pattern generator model inspired by the neural circuits controlling the locomotion in the lamprey’s spinal cord.

The emphasis in the reported works in the literature, have focused in achieving either forward or constant turning locomotion in the path description. The combination of a time-varying curvature and heading description of the path that needs to be followed by a snake is the natural extension to the reported research. Very few works have focused on this problem, due to the lack of theoretical control tools, or, because of the problem’s complexity. The trajectory tracking of snake robots, where few joints/links are wheeled is considered in [16]. [17] proposes a waypoint guidance strategy for steering a snake robot along a path, defined by straight line interconnected waypoints. Additionally, a motion planning framework using a three-dimensional spline curve passing through prescribed interpolation points, based on fitting the snake robot’s kinematic structure, is proposed in [18].

Anthony Tzes is with the Department of Electrical & Computer Engineering, University of Patras, Rio, Achaia-26500, Greece.

Eleni Kelasidi was with the Electrical and Computer Engineering Department, University of Patras, Greece. She is now with the Norwegian University of Science and Technology, Department of Engineering Cybernetics, Trondheim, Norway.

Corresponding author’s email: eleni.kelasidi@itk.ntnu.no

In this paper, a tracking controller is proposed for a wheel-less planar snake-like robot. The robot is dictated to follow a curvature and heading based parametrized curve. The resulting robot's path is a homothet to the desired path. Simulation results are presented, illustrating the performance of the proposed tracking controller for circle and spiral curves.

The paper is organized as follows. Section II presents the dynamic model of a planar snake robot. The proposed tracking controller is outlined in Section III, while simulation results are presented in Section IV. Finally, conclusions and suggestions for further research are given in Section V.

## II. DYNAMIC MODEL OF A PLANAR SNAKE ROBOT

This section presents a model of the dynamics of a 2D-snake robot moving on a flat surface; the notation follows along the works of [4, 19]. The snake robot consists of  $n$  links of equal length  $2l = 2l_i, i = 1, \dots, n$  interconnected by  $n - 1$  joints. The links are assumed to have the same mass  $m_i$  and moment of inertia  $J = \frac{1}{3}m_i l_i^3$ . Each link has a uniformly distributed mass density. The total mass of the snake robot is defined as  $m = \sum_{i=1}^n m_i$ . The coordinates of the center of gravity of  $i$ th link and the angle between the link and the  $x$ -axis are defined as  $(x_i, y_i)$  and  $\theta_i$ , respectively. Define

$$A = \begin{bmatrix} 1 & 1 & & & \\ & \ddots & \ddots & & \\ & & & 1 & 1 \\ & & & & & 1 & -1 \end{bmatrix}, D = \begin{bmatrix} 1 & -1 & & & \\ & \ddots & \ddots & & \\ & & & 1 & -1 \end{bmatrix},$$

where  $A, D \in \mathbb{R}^{(n-1) \times n}$ . Furthermore,

$$e = [1 \quad \dots \quad 1]^T \in \mathbb{R}^n, E = \begin{bmatrix} e & 0_{n \times 1} \\ 0_{n \times 1} & e \end{bmatrix} \in \mathbb{R}^{2n \times 2},$$

$$\sin \theta = [\sin \theta_1 \quad \dots \quad \sin \theta_n]^T \in \mathbb{R}^n,$$

$$S_\theta = \text{diag}(\sin \theta) \in \mathbb{R}^{n \times n},$$

$$\cos \theta = [\cos \theta_1 \quad \dots \quad \cos \theta_n]^T \in \mathbb{R}^n,$$

$$C_\theta = \text{diag}(\cos \theta) \in \mathbb{R}^{n \times n},$$

$$\text{sign} \theta = [\text{sign} \theta_1 \quad \dots \quad \text{sign} \theta_n]^T \in \mathbb{R}^n,$$

$$\dot{\theta}^2 = [\dot{\theta}_1^2 \quad \dots \quad \dot{\theta}_n^2]^T \in \mathbb{R}^n,$$

$$J = \text{diag}(J_1, \dots, J_n), M = \text{diag}(m_1, \dots, m_n),$$

$$L = \text{diag}(l_1, \dots, l_n), H = LA'(DM^{-1}D')AL,$$

$$N = M^{-1}D'(DM^{-1}D')^{-1}AL, \mathcal{J} = J + S_\theta H S_\theta + C_\theta H C_\theta,$$

$$\mathcal{C} = S_\theta H C_\theta - C_\theta H S_\theta, \mathcal{L} = [S_\theta N' \quad -C_\theta N']'.$$

### A. Simplified Viscous Friction Description

For the simplified viscous friction dynamic modeling, the expressions for the total friction force  $f$  and total torque  $\tau$  must be defined in terms of  $x, y$  and  $\theta$ . The total torque-vector's,  $\tau \in \mathbb{R}^n$ ,  $i$ th entry is  $\tau_i$ , and similarly  $f_x, f_y \in \mathbb{R}^n$ , where  $(f_x, f_y)$  are the  $(x, y)$  components of the friction

force vector  $f_i$ . The total friction force vector  $f$  and the position vector  $z$  are defined by:

$$f = \begin{bmatrix} f_x \\ f_y \end{bmatrix}, z = \begin{bmatrix} x \\ y \end{bmatrix}. \quad (1)$$

The total friction force (2) and torque (3), based on a simplified viscous snake-to-ground friction term [4], acting on the system can be expressed as:

$$f = -\Omega_\theta D_f \Omega'_\theta \dot{z}, \quad (2)$$

$$\tau = -D_\tau \dot{\theta}, \quad (3)$$

where

$$D_f = \begin{bmatrix} C_t M & 0 \\ 0 & C_n M \end{bmatrix}, D_\tau = C_n J, \Omega_\theta = \begin{bmatrix} C_\theta & -S_\theta \\ S_\theta & C_\theta \end{bmatrix}, \\ C_t = \text{diag}(c_{1,t}, \dots, c_{n,t}), C_n = \text{diag}(c_{1,n}, \dots, c_{n,n}), \quad (4)$$

where  $c_{i,t}$  ( $c_{i,n}$ ) correspond to the tangential (normal) viscous friction coefficient for the  $i$ th link,  $i = 1, \dots, n$ .

### B. Dynamic Equations of Motion

The snake robot has  $n + 2$  degrees of freedom, and  $3n$  variables are used ( $x, y$ , and  $\theta$ ) to describe its motion. Parameters  $u$  and  $w$  (5) correspond to the joint applied torques from the actuators and the position of the snake's center of gravity, respectively [4].

$$w = \begin{bmatrix} w_x \\ w_y \end{bmatrix} = \frac{1}{m} \begin{bmatrix} e' M x \\ e' M y \end{bmatrix}. \quad (5)$$

The overall set of dynamic equations of motion can be assembled into the following:

$$\begin{bmatrix} \mathcal{J} & 0 \\ 0 & mI \end{bmatrix} \begin{bmatrix} \ddot{\theta} \\ \ddot{w} \end{bmatrix} + \begin{bmatrix} C \dot{\theta}^2 \\ 0 \end{bmatrix} + \\ \begin{bmatrix} \mathcal{R} & \mathcal{S} \\ \mathcal{S}' & \mathcal{Q} \end{bmatrix} \begin{bmatrix} \dot{\theta} \\ \dot{w} \end{bmatrix} = \begin{bmatrix} D' \\ 0 \end{bmatrix} u, \quad (6)$$

where

$$\begin{bmatrix} \mathcal{R} & \mathcal{S} \\ \mathcal{S}' & \mathcal{Q} \end{bmatrix} = \begin{bmatrix} D_\tau & 0 \\ 0 & 0 \end{bmatrix} + \begin{bmatrix} \mathcal{L}' \\ E' \end{bmatrix} \Omega_\theta D_f \Omega'_\theta [ \mathcal{L} \quad E ]. \quad (7)$$

## III. INNER/OUTER LOOP CONTROL ARCHITECTURE

The mathematical expression for the snake's gait in locomotion studies depend on its construction and model. Lateral undulation [3] is the fastest and most common form of snake locomotion, where the motion is achieved by creating continuous body waves that are propagated backwards from head to tail. In order to achieve the lateral undulation, the snake is commanded to follow the serpenoid curve [2]. The proposed lateral undulation is realized by controlling each joint of the snake robot according to the sinusoidal reference

$$\varphi_i^* = a \sin(\omega t + (i - 1)\beta) + \gamma, i = 1, \dots, n - 1, \quad (8)$$

where the parameter  $a$  corresponds to the amplitude of the serpentine wave that propagates along the body of the snake robot,  $\eta = \omega t$ ,  $\beta$  determines the phase shift between the sequential joints, and  $\gamma$  is a joint offset that is used to control

the direction of the motion. The parameters  $a$  and  $\beta$  are typically fixed and the parameters  $\omega, \gamma$  are used to control the speed and the direction of the snake robot. An inner loop PD-controller is used for trajectory tracking attempting to compensate the effects of the snake's dynamics, while an outer-loop first-order controller is used for the formation of the reference joint angles by tracking the desired heading and velocity, as shown in Figure 1.

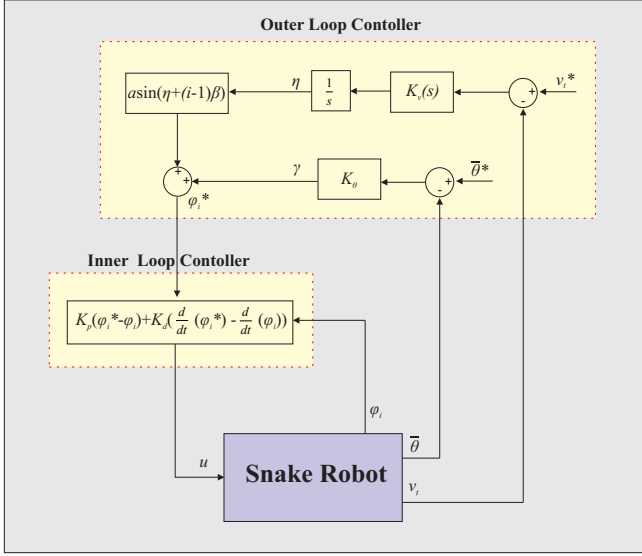


Fig. 1: Controller Structure

### A. Reference Trajectory

Allowing the robot to track a homothet of the reference trajectory  $(x_r(t), y_r(t))$ , a reference tangential velocity  $v_t^*(t)$  and a reference tangential angle  $\bar{\theta}^*(t)$  are needed [20], as

$$\bar{\theta}^*(t) = \arctan(\dot{y}_r(t), \dot{x}_r(t)), \quad (9)$$

$$v_t^*(t) = \pm \sqrt{\dot{y}_r^2(t) + \dot{x}_r^2(t)}, \quad (10)$$

where the positive(negative) sign of  $v_t^*(t)$  refers to the forward(backward) movement.

For the case, where the reference trajectory corresponds to a circle (center, radius)=[ $x_0, y_0$ ],  $R$ ), then  $x_r = x_0 + R \cos(\omega_f t)$  and  $y_r = y_0 + R \sin(\omega_f t)$ , the expressions of the heading angle and the tangential velocity, in clockwise direction, are

$$\bar{\theta}^*(t) = \arctan(\dot{y}_r(t), \dot{x}_r(t)) = \omega_f t - \pi/2, \quad (11)$$

$$v_t^*(t) = \sqrt{\dot{y}_r^2(t) + \dot{x}_r^2(t)} = \dot{\theta}^*(t)R = \omega_f R, \quad (12)$$

where the  $\dot{\theta}^*(t)$  is the angular velocity.

Similarly, for a spiral curve with general equations  $x_r = x_0 + r(t) \cos(\omega_f t)$  and  $y_r = y_0 + r(t) \sin(\omega_f t)$ , the heading angle and tangential velocity are:

$$\bar{\theta}^*(t) = \arctan\left(\frac{\dot{r}(t) \sin(\omega_f t) + r(t) \omega_f \cos(\omega_f t)}{\dot{r}(t) \cos(\omega_f t) - r(t) \omega_f \sin(\omega_f t)}\right) \quad (13)$$

$$v_t^*(t) = \dot{\theta}^*(t)r(t). \quad (14)$$

### B. Outer Loop Controller

The outer loop controller is responsible for the formation of the reference joint angles by tracking the desired heading and velocity. The orientation  $\bar{\theta}$  (15) of the robot is denoted as the average of the link angles, while  $v_t$  (16) is the speed of the snake's center of gravity in the local  $\bar{\theta}$  direction, where

$$\bar{\theta} = \frac{1}{n} \sum_{i=1}^n \theta_i \quad (15)$$

$$v_t = \dot{w}_x \cos(\bar{\theta}) + \dot{w}_y \sin(\bar{\theta}). \quad (16)$$

Let the speed(directional) error be  $v_t^* - v_t (\bar{\theta}^* - \bar{\theta})$ , and consider the parameters  $\eta$  (17) and  $\gamma$  (18) as responsible for the appropriate transformation of the command motion the reference angle of the  $i$ th joint  $\varphi_i^*$ . The following proportional-integral controller is applied

$$\eta = \frac{1}{s} \left[ K_1 + \frac{K_2}{s} \right] (v_t^* - v_t), \quad (17)$$

$$\gamma = K_\theta (\bar{\theta}^* - \bar{\theta}). \quad (18)$$

The structure of the suggested controller [4] is responsible for the zero steady state tracking error  $v_t^* - v_t$ .

### C. Inner Loop Controller

A standard proportional-derivative (PD) controller is used to generate the joint actuation torques so that the actual motion  $\varphi_i = \theta_i - \theta_{i+1}$  follows the reference signal  $\varphi_i^*$ . The  $i$ th joint's PD controller is

$$u_i = K_{p,i}(\varphi_i^* - \varphi_i) + K_{d,i}(\dot{\varphi}_i^* - \dot{\varphi}_i), \quad (19)$$

where  $K_{p,i}$  and  $K_{d,i}$  are the gains of the PD controller.

In snake-robot control design the selection of the inner loop and outer loop gains relies on an ad-hoc procedure. These gains are related to the performance of the snake's in traversing the desired trajectory. It should be noted that the resulting trajectory's shift depends on the initial error between the snake and the trajectory. In general, large gains result in a faster performance, at the expense of needing large torques at the actuators. The innovation in the suggested controller amounts to the combination of the inner/loop control structure and the need to obtain an expression for a velocity/heading parametrized curve. In previous works, either straight lines, or paths with constant angular velocity (i.e., circles) had been examined and very few ad-hoc attempts have been recorded for general paths.

## IV. SIMULATION STUDIES

The performance of the guidance strategy proposed in Section III is investigated in simulation studies for various easy (circle) and time-varying curvature (difficult) curve-following cases. A snake robot (close to the one of the UPAT - snake prototype shown in Figure 2) was considered with  $n = 5$  links, each one having length  $2l_i = 0.102m$  and mass  $m_i = 0.5kg$ . The initial values of all states of the snake robot were set to zero. The friction related parameters in the tangential(normal direction) were set as  $c_{i,t} = 0.1$  and  $c_{i,n} = 10$ . The selected PD-controller parameters are

$K_p = 200, K_d = 10$  and the gait parameters correspond to  $\alpha = \pi/3$  and  $\beta = 2\pi/n$ .

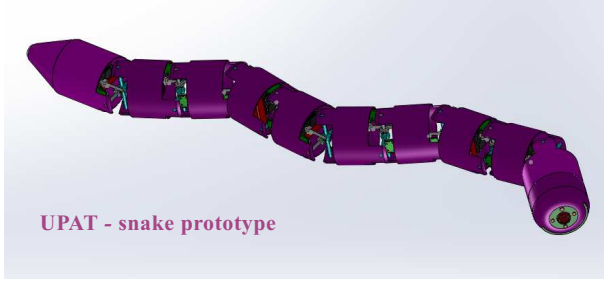


Fig. 2: UPAT – snake prototype

### A. Circle Tracking Study

As discussed in Section III, for the movement of the snake robot in circular trajectory, it is sufficient to adjust the control signal in (8) by incorporating the heading and the linear velocity of the robot. If a controller is adopted for handling only the heading of the robot, with its controller parameter  $K_\theta = -1$  while  $\omega$  is fixed. In this case, the snake-robot performs a circular trajectory, but its linear velocity and the resulting circle's radius is uncontrollable. For the noted parameters, the resulting angular velocity  $\omega_f$  was 0.2 rad/sec. If the parameter  $\omega$  from (8), is doubled, then the snake robot is moving over a circle of double radius (for  $\omega = 3$  rad/sec,  $R_1 = 0.7537$  m,  $(x_0, y_0) = (0.0049, 0.7564)$ , as shown in Figure 3 and for  $\omega = 6$  r/sec,  $R_2 = 1.5851$  m,  $(x_0, y_0) = (-0.0609, 1.5870)$ , as shown in Figure 4). The final tangential velocity was also doubled, since for  $\omega = 3$  rad/sec,  $v_{t_1} = 0.1507$  m/sec, as shown in Figure 5 while for  $\omega = 6$  r/adsec,  $v_{t_2} = 0.3169$  m/sec, as shown in Figure 6).

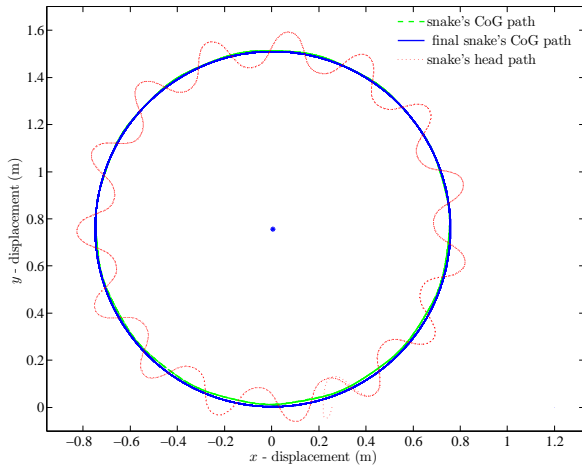


Fig. 3: Circle path heading-tracking ( $\omega = 3$  rad/sec)

In the previous case only the direction of the robot was controlled, and if both velocity and heading are to be tracked, a controller with parameters set at  $K_1 = 49.962, K_2 = 18.042$ , and  $K_\theta = -1$ , was applied with a reference tangential velocity of  $v_t^* = 0.2$  m/sec for a reference circle path ( $R = 0.5$  m and  $\omega_f = 0.4$  rad/sec). The snake's

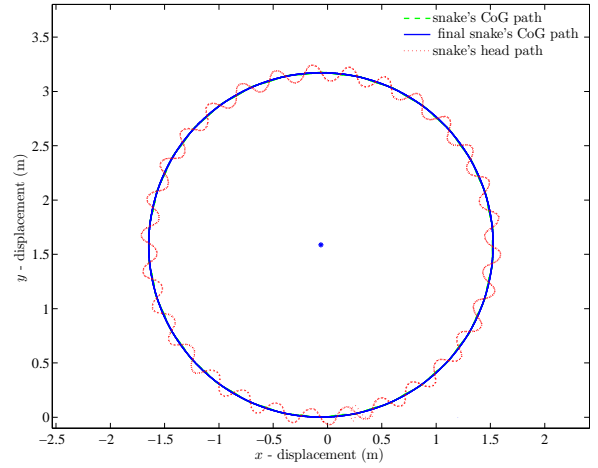


Fig. 4: Circle path heading-tracking ( $\omega = 6$  rad/sec)

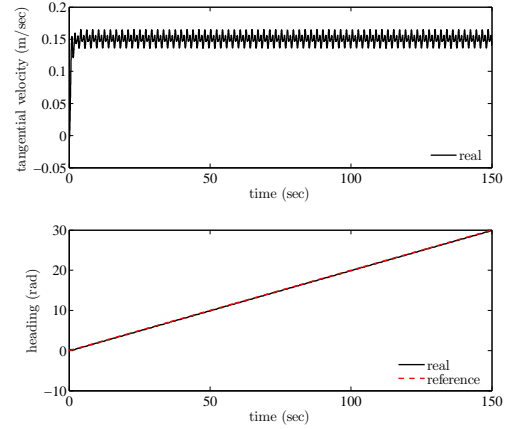


Fig. 5: Snake robot's tangential velocity and heading (circle case, heading tracking) portion ( $\omega = 3$  rad/sec)

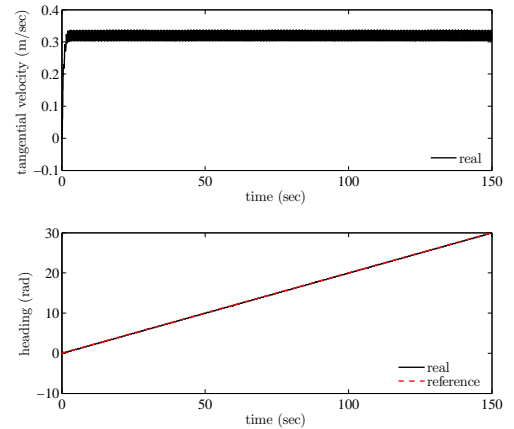


Fig. 6: Snake robot's tangential velocity and heading (circle case, heading tracking) portion ( $\omega = 6$  rad/sec)

response is shown in Figure 7 illustrating the effectiveness of the proposed control law. In another case, for parameters

$K_1 = 41,635, K_2 = 9.021, K_\theta = -0.5$ , with a reference tangential velocity  $v_t^* = 0.2$  m/sec, for a reference circle path ( $R = 5$  m and  $\omega_f = 0.04$  r/sec), the snake's response is highlighted in Figure 8. In the steady periodic (Poincare-map) state, the snake's center of gravity moves over a circle of  $0.5+0.0017$  m for the first case and at a circle with radius error of  $0.0009$  m for the second ( $5$  m) circle's radius case.

The primary cause of the shifting of the center of the circle is due to the time needed for the snake to accelerate in order to track the circular-path. The relative small errors in the  $x$  and  $y$ -axis are also presented in the middle portion of Figures. 7 and 8, indicating the efficiency of the suggested algorithm.

### B. Spiral Curve Tracking Study

Several snake control methods have been developed for motion over a circular trajectory developed [6,16]. The spiral-curve tracking problem is considered to be a superset of the (simple) circle tracking study. In this case, the controller's parameters were selected as  $K_1 = 166.54, K_2 = 54.126, K_\theta = -2, v_t^* = 0.2$  m/sec and  $\omega_f = 0.2$  rad/sec for a spiral trajectory of radius  $r(t) = \sqrt{t}$  shown in Figure 9 (left)). For a different spiral case of radius  $r(t) = t$ , the selected parameters were  $K_1 = 58.289, K_2 = 45.105, K_\theta = -1, v_t^* = 0.2$  m/sec and  $\omega_f = 0.2$  rad/sec shown in Figure 10 (left)). In both cases, the snake robot manages to achieve an almost zero steady state error in tangential velocity and direction with a very fast response as shown in the right portion of Figures 9 and 10. Again, the shift present in these Figures is because of the initial error in the snake's velocity and heading.

## V. CONCLUSIONS

The trajectory control problem for a wheel-less planar snake robot, with active joints, based on a dynamic model [4] that includes viscous friction, is considered in this article. Taking into account the philosophy behind the adoption of the snake's serpentine motion, a simple method has been proposed for the heading direction and tangential velocity control. The presented simulation studies illustrate the effectiveness of the proposed guidance strategy.

## ACKNOWLEDGMENTS

This research was supported in part by the 'John S. Latsis Public Benefit Foundation', Greece, 2010-2011.

## REFERENCES

- [1] J. Gray, "The mechanism of locomotion in snakes," *J.Exp.Biol.*, vol. 23, no. 2, pp. 101-120, 1946.
- [2] S. Hirose, *Biologically inspired robots : snake-like locomotors and manipulators*. Oxford University Press, Oxford, New York, 1993.
- [3] A. A. Transeth and K. Y. Pettersen, "Developments in snake robot modeling and locomotion," in *Proc. 9th Int. Conf. Control, Automation, Robotics and Vision ICARCV '06*, 2006, pp. 1-8.
- [4] M. Saito, M. Fukaya, and T. Iwasaki, "Serpentine locomotion with robotic snakes," *Control Systems, IEEE*, vol. 22, no. 1, pp. 64-81, 2002.
- [5] P. Wiriyacharoensunthorn and S. Laowattana, "Analysis and design of a multi-link mobile robot (serpentine)," in *Industrial Technology, 2002. IEEE ICIT '02. 2002 IEEE International Conference on*, vol. 2, Dec. 2002, pp. 694-699 vol.2.

- [6] C. Ye, S. Ma, B. Li, and Y. Wang, "Turning and side motion of snake-like robot," in *Proc. IEEE Int. Conf. Robotics and Automation ICRA '04*, vol. 5, 2004, pp. 5075-5080.
- [7] M. Ishikawa, "Iterative feedback control of snake-like robot based on principal fiber bundle modeling," *International Journal of Advanced Mechatronic Systems*, vol. 1, no. 3, pp. 175-182, 2009.
- [8] M. Ishikawa, K. Owaki, M. Shinagawa, and T. Sugie, "Control of snake-like robot based on nonlinear controllability analysis," in *Proc. IEEE Int Control Applications (CCA) Conf.*, 2010, pp. 1134-1139.
- [9] P. Liljeback, K. Y. Pettersen, O. Stavdahl, and J. T. Gravdahl, "Controllability and stability analysis of planar snake robot locomotion," *IEEE Trans. Automat. Contr.*, vol. 56, no. 6, pp. 1365-1380, 2011.
- [10] P. Liljeback, I. U. Haugstuen, and K. Y. Pettersen, "Path following control of planar snake robots using a cascaded approach," *IEEE Trans. Contr. Syst. Technol.*, vol. 20, no. 1, pp. 111-126, 2012.
- [11] J. Liu, Y. Wang, B. Li, and S. Ma, "Path planning of a snake-like robot based on serpenoid curve and genetic algorithms," in *Proc. Fifth World Congress Intelligent Control and Automation WCICA 2004*, vol. 6, 2004, pp. 4860-4864.
- [12] C. Ye, D. Hu, S. Ma, and H. Li, "Motion planning of a snake-like robot based on artificial potential method," in *Proc. IEEE Int Robotics and Biomimetics (ROBIO) Conf.*, 2010, pp. 1496-1501.
- [13] X. Wu and S. Ma, "Autonomous collision-free behavior of a snake-like robot," in *Proc. IEEE Int Robotics and Biomimetics (ROBIO) Conf.*, 2010, pp. 1490-1495.
- [14] M. Ghayour, N. Negahbani, and A. H. Nakhaei, "Controlling wheel less snake-like robot by considering the coulomb elliptical friction model and utilizing the path of serpenoid curve," in *Proc. IEEE Int. Symp. Industrial Electronics ISIE 2009*, 2009, pp. 175-182.
- [15] A. Ijspeert and A. Crespi, "Online trajectory generation in an amphibious snake robot using a lamprey-like central pattern generator model," in *Proc. IEEE Int Robotics and Automation Conf.*, 2007, pp. 262-268.
- [16] F. Matsuno and H. Sato, "Trajectory tracking control of snake robots based on dynamic model," in *Proc. IEEE Int. Conf. Robotics and Automation ICRA 2005*, 2005, pp. 3029-3034.
- [17] P. Liljeback and K. Y. Pettersen, "Waypoint guidance control of snake robots," in *Proc. IEEE Int Robotics and Automation (ICRA) Conf.*, 2011, pp. 937-944.
- [18] G. Ford, R. Primerano, and M. Kam, "Crawling and rolling gaits for a coupled-mobility snake robot," in *Proc. 15th Int Advanced Robotics (ICAR) Conf.*, 2011, pp. 556-562.
- [19] P. Liljeback, K. Y. Pettersen, O. Stavdahl, and J. T. Gravdahl, "Hybrid modelling and control of obstacle-aided snake robot locomotion," *IEEE Transactions on Robotics*, vol. 26, no. 5, pp. 781-799, 2010.
- [20] S. M. LaValle, *Planning Algorithms*. Cambridge, U.K.: Cambridge University Press, 2006.

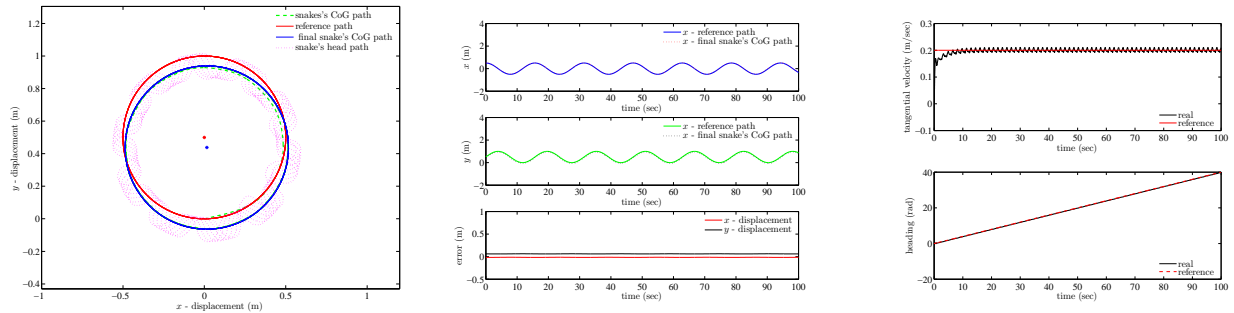


Fig. 7: Circle case tracking ( $R = 0.5\text{m}$ : path,  $x$  and  $y$  axis time, and velocity/heating response)

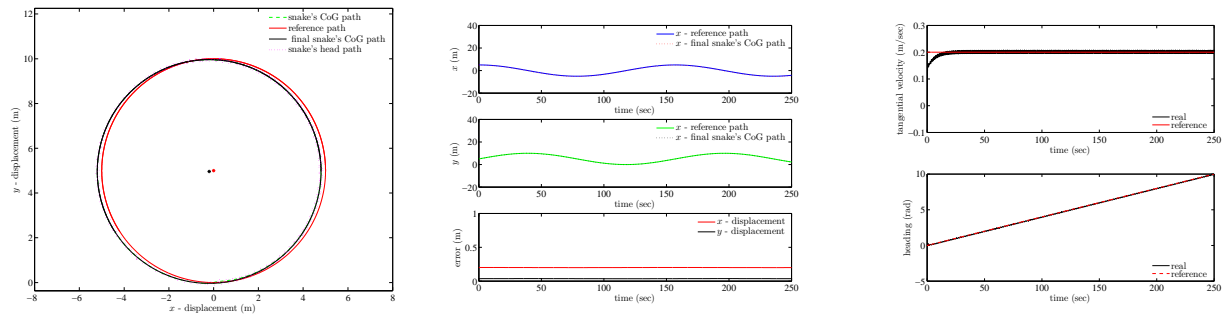


Fig. 8: Circle case tracking ( $R = 5\text{m}$ : path,  $x$  and  $y$  axis time, and velocity/heating response)

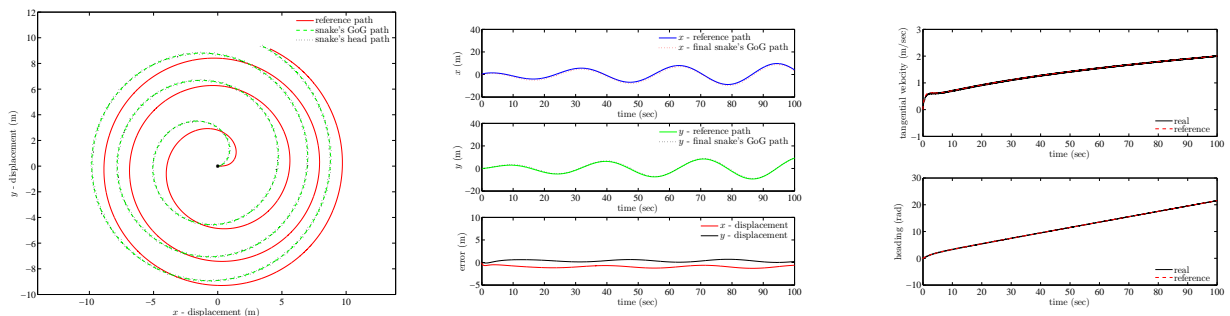


Fig. 9: Spiral case tracking ( $r(t) = \sqrt{t}$  m: path,  $x$  and  $y$  axis time, and velocity/heating response)

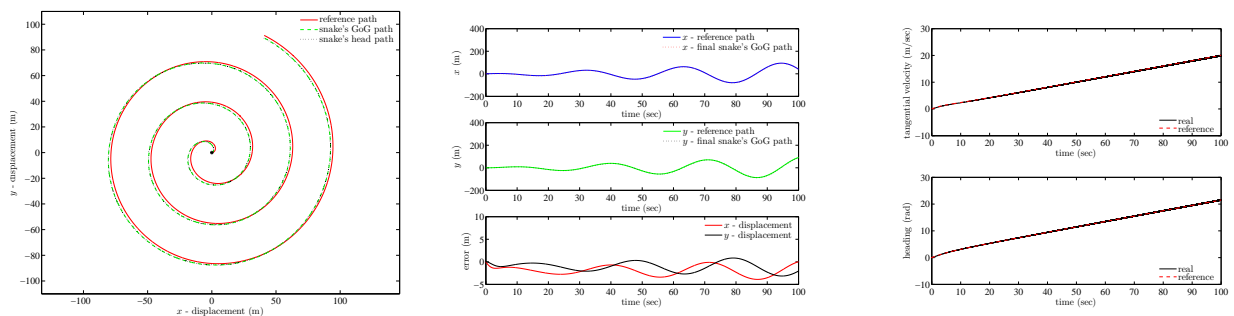


Fig. 10: Spiral case tracking ( $r(t) = t$  m: path,  $x$  and  $y$  axis time, and velocity/heating response)